ACS OMEGA

http://pubs.acs.org/journal/acsodf

Article

Future Paradigm of 3D Printed Ni-Based Metal Organic Framework Catalysts for Dry Methane Reforming: Techno-economic and Environmental Analyses

Jia Ling Ong, Adrian Chun Minh Loy, Sin Yong Teng, and Bing Shen How*

Cite This: *ACS Omega* 2022, 7, 15369−15384

Read Online

ACCESS | Metrics & More | Article Recommendations | Supporting Information

ABSTRACT: Dry reforming of biogas is referred as an attractive path for sustainable H_2 production over decades. Meanwhile, in the Malaysian context, the abundance of palm oil mill effluent (POME) produced annually is deemed as a potential renewable source for renewable energy generation. Conventionally, nickel (Ni) is the most common catalyst used in the industrial-scale dry reforming of methane (DRM) to yield H_2, but it is subject to the drawbacks of sintering and deactivation after a long reaction time at high temperatures (>500 °C). Therefore, this work aims to provide an insight on the feasibility of the application of modified Ni-based catalysts in DRM, specifically in the economic and environmental aspects. From the benchmarking study of various Ni-based catalysts (e.g., bimetallic (Ni-Ce/Al_2O_3), alumina support (Ni/Al_2O_3), protonated titanate nanotube (Ni-HTNT), and unsupported), the Ni-MOF catalyst, notably, had proven its prominence in both economic and environmental aspects on the same basis of 10 tonnes of H_2 production. The MOF-based catalyst not only possessed a better economic performance (net present value 61.86%, 140%, and 563.08% higher than that of Ni-Ce/Al_2O_3, Ni/Al_2O_3, and Ni-HTNT) but also had relatively lower carbon emissions (13.18%, 20.09%, and 75.72% lower than that of Ni/Al_2O_3, Ni-HTNT, and unsupported Ni). This work also accounted for 3D printing technology for the mass production of Ni-MOF catalysts, where the net present value was 2 to 3% higher than that of the conventional production method. Additionally, sensitivity analysis showed that the H_2 price has the greatest impact on the feasibility of DRM as compared to other cost factors.

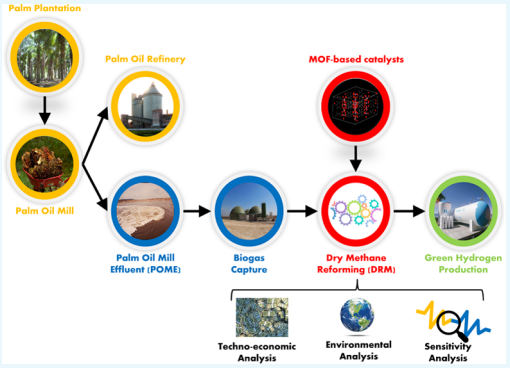

1. INTRODUCTION

Over the decades, H_2 demand has increased rapidly alongside the growth of other hydrogen-sink industries (e.g., petroleum refining, fine-chemical production, and power generation).[1−3] The H_2 production had increased over the years and achieved 73.3 million tonnes in 2020 and aimed to reach 300 million tonnes by 2030, as stated by S&P Global Platts and Statistica.[4,5] Despite H_2 being classified as a promising energy carrier, its production is still emitting *ca.* 830 million tonnes of CO_2 per year due to its derivation *via* fossil fuels.[6] A greener solution that can fulfill the high H_2 global demand without impeding the environmental sustainability is highly essential. This is, in fact, aligned with the seventh and eighth Sustainable Development Goals (SDGs) that emphasize the importance of (i) clean and affordable energy production for the world and (ii) mitigation of global climate change issues.[7]

Malaysia, being the second largest palm oil producer in the world, is continuously contributing more than a quarter of the global palm oil production (*ca.* 26%, 19.7 Mt per year).[8,9] This phenomenon led to an enormous amount of palm oil mill effluent (POME) generation as waste (e.g., 2 to 3.5 times of crude palm oil). It can be treated *via* anaerobic digestion to produce biogas (consists of about 50−75% of CH_4 and 25−45% of CO_2), which is deemed as a green source for H_2 production.[10,11] In conjunction to reducing carbon emissions and promoting biomass valorization, green H_2 production from biogas becomes an attractive and greener option to fulfill the escalating H_2 demand, tackling the waste management issue as well as favoring the "waste to wealth" strategy.[12]

Dry reforming of methane (DRM) is one of the technologies that is capable of converting biomass into valuable H_2. From Table 1 (i.e., the possible reactions in the DRM process), most of the reactions favoring the production of H_2 are endothermic, in which a high temperature (>650 °C) is essential. However, after a long period of reaction time, most of the commercial catalysts (e.g., Ni, Co, Zeolite, Mg, Na, and Cu) will suffer from deactivation due to coke deposition and poisoning.[13−15] To

Received: December 5, 2021
Accepted: April 12, 2022
Published: April 26, 2022

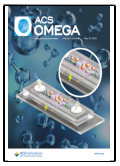

https://doi.org/10.1021/acsomega.1c06873
ACS Omega 2022, 7, 15369−15384

Table 1. Occurrence of Reactions in the DRM process[17]

type of reaction	reaction	heat of reaction
CO_2 reforming of methane	$CH_4 + CO_2 \leftrightarrow 2H_2 + 2CO$	ΔH° = 260.5 kJ/mol
reverse water–gas shift (RGWS)	$CO_2 + H_2 \leftrightarrow CO + H_2O$	ΔH° = 41.0 kJ/mol
steam reforming of methane	$CH_4 + H_2O \leftrightarrow CO + 3H_2$	ΔH° = 206.0 kJ/mol
steam reforming of methane	$CH_4 + 2H_2O \leftrightarrow CO_2 + 4H_2$	ΔH° = 165.0 kJ/mol
combustion of methane	$CH_4 + 2O_2 \leftrightarrow CO_2 + 2H_2O$	ΔH° = −802.0 kJ/mol
partial oxidation of methane	$CH_4 + 0.5O_2 \leftrightarrow CO + 2H_2$	ΔH° = −36.0 kJ/mol
methane decomposition	$CH_4 \leftrightarrow 2H_2 + C$	ΔH° = 75.0 kJ/mol
Boudouard/disproportionation reaction	$2CO \leftrightarrow CO_2 + C$	ΔH° = −172.5 kJ/mol
CO hydrogenation/reduction	$H_2 + CO \leftrightarrow C + H_2O$	ΔH° = −131.5 kJ/mol

increase the life span and catalytic activity of the catalyst, noble metals (e.g., Pt, Pd, and Ru) are often used as a co-catalyst alongside the non-noble metals. Despite having excellent resistance toward coking, noble metal catalysts are often expensive and earth-scarce, hindering their attractiveness to be used in bulk quantities.[16]

Comparatively, among non-noble metals (e.g., nickel, copper, and cobalt), Ni-based catalysts have been extensively used in industrial applications due to their affordable cost and decent catalytic performance. For instance, García-Diéguez et al.[18] had incorporated Ni and Pt at different ratios and discovered that $0.4Pt_4Ni/Al_2O_3$ had the best performance of CH_4 conversion of 70% and CO_2 conversion of 75% at 700 °C. In addition, Chein and Fung[19] also reported that bimetallic catalysts such as doping ceria to nickel ($Ni\text{-}Ce/Al_2O_3$) have improved the catalytic performance where the CH_4 conversion had increased from 76 to 82% and CO_2 conversion had increased to 88% from 78%.[19] Figure 1 shows the timeline of the development of Ni-based catalysts from 1928 until the present, from monometallic, the introduction of promoters and supports, bimetallic, mesoporous matrix to Ni-based MOF.

Over the last decade, the synthesis of nano-engineered metal–organic frameworks (MOFs) has shown a tremendous development with reassuring application in catalysis processes, aligning with the Principles of Green Chemistry of ″Design of Energy Efficiency″, ″Use of Renewable Feedstocks″, and ″Catalysis″.[26,27] Due to the unique features such as intrinsic porosity, large surface area, tunable characteristic, long life span, and low density, MOFs are expected to offer desired improvements in contemporary organic chemistry and modern organometallic catalysis.[28,29] One of the most promising approaches for the application of MOF-based heterogeneous catalysts is thermal carbonization, including pyrolysis, DRM, and Fischer–Tropsch synthesis.[30] MOFs have been introduced into the carbonization field, where these hybrid materials are used as sacrificial templates. This overcomes the shortcomings of conventional catalysts, such as (1) short life span due to coking, (2) low surface area-active sites for enhancing the carbonization reaction, and (3) nonhomogeneous dispersion of metal sites.[31,32] The first study that reported on the incorporation of MOF into Ni-based catalysts for the DRM process can be dated back to 2019 in the study by Chin et al.[33] They had prepared a bimetallic (Ni-Ce) MOF-derived catalyst in the DRM process and proved that the application of MOF as a precursor improved its catalytic performance as the MOF application had successfully produced higher-dispersed particles. It is then followed by Karam et al.,[25] who have synthesized a highly porous Ni-Al/MOF MIL-53 for the DRM reaction in 2020. Notably, the Ni-Al/MOF MIL-53 was still highly active after 100 h of reaction and managed to yield 3 times higher CO_2 and CH_4 conversions than those of the conventional Ni/Al catalyst. Given the aforementioned unique features of MOF, the MOF-derived catalysts had proven the capability of offering greater (about 2 to 3 times) CO_2 and CH_4 conversions as compared to the conventional Ni-based catalysts (Ni impregnated on γ-alumina).

To the best of the authors' knowledge, the existing work by Karam et al.[25] in 2020 merely focused on the proof-of-concept experimental work for the feasibility of Ni-based MOF catalysts for DRM processes. None of the literature has reviewed the respective overall techno-economic and environmental performances. Therefore, this research attempts to provide an overview of the economic and environmental feasibility of the application

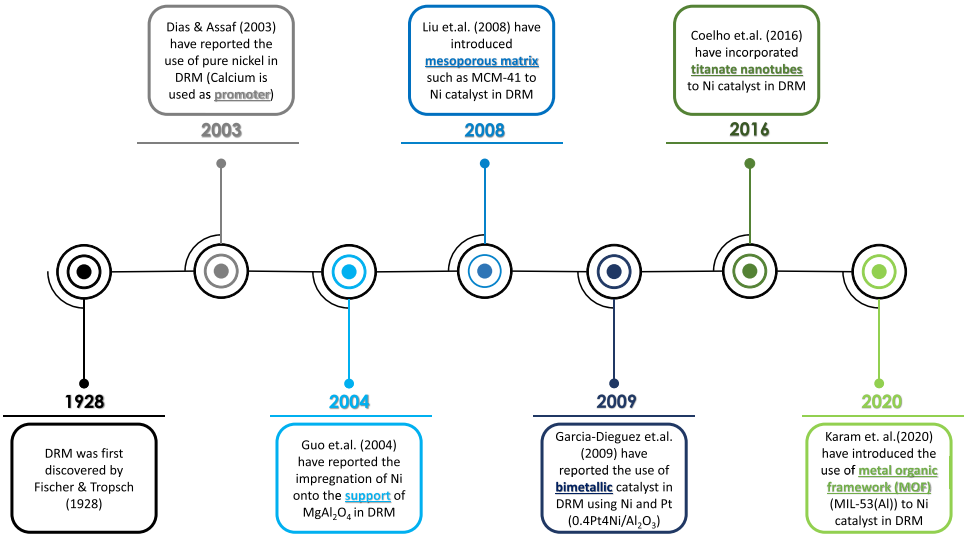

Figure 1. Timeline of Ni-based catalytic DRM revolution.[18,20−25]

https://doi.org/10.1021/acsomega.1c06873
ACS Omega 2022, 7, 15369−15384

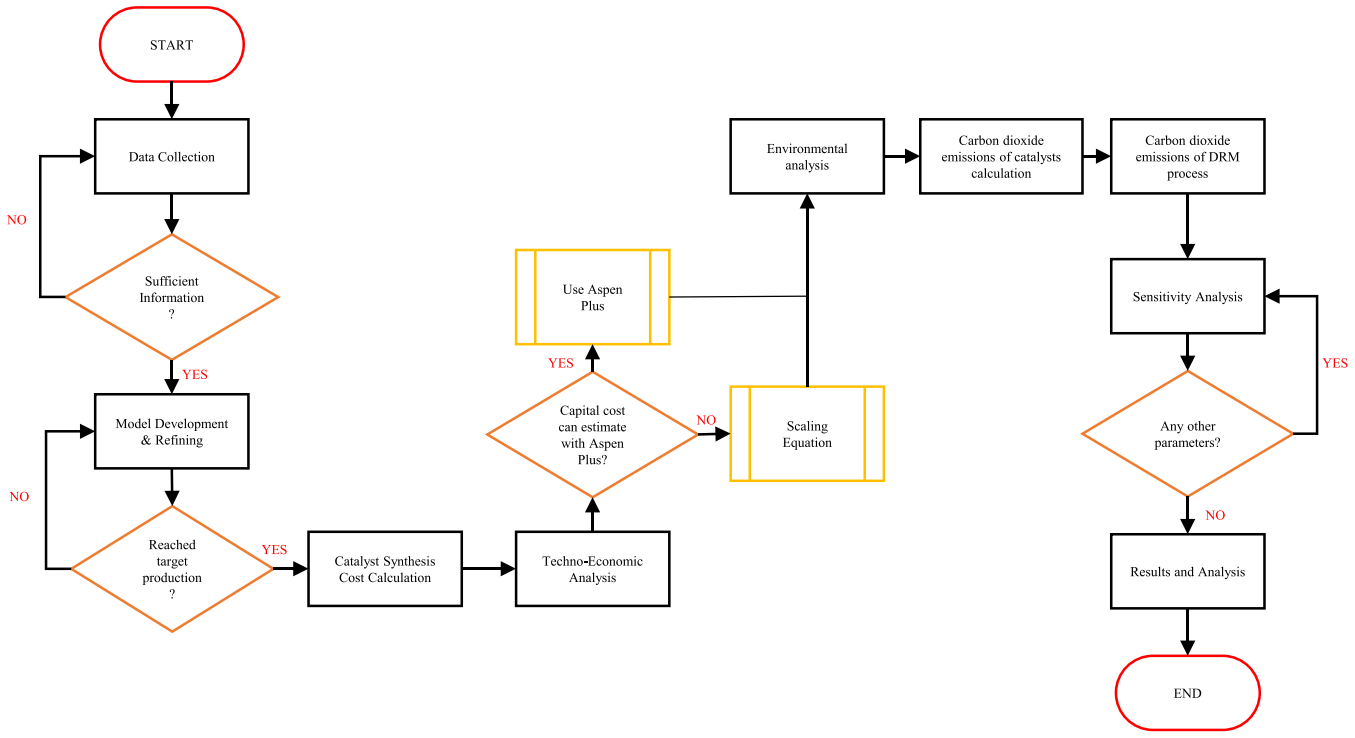

(a)

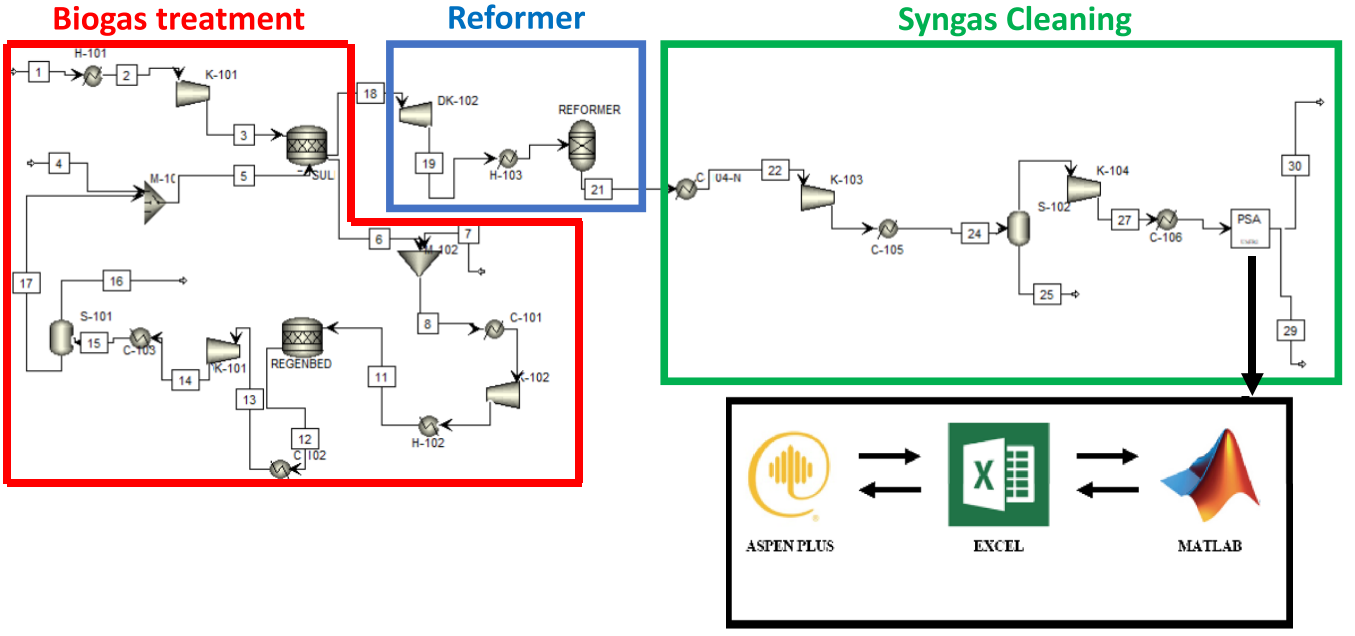

(b) (c)

Figure 2. Illustrative diagram for the (a) research methodology flow; (b) model development of DRM process using Aspen Plus V12; and (c) model development of PSA via integration of Aspen Plus V12, Microsoft Excel, and MATLAB R2019b.

of Ni-MOF-based catalysts for the DRM process. Alongside the conventional way of catalyst preparation, this work also discusses the possibility of the adoption of additive mass production for Ni-MOF-based catalysts *via* a cutting-edge 3D printing method. Herein, given the low technology readiness level (TRL) of the application of MOF in DRM, this study can be considered as the first preliminary economic and environmental assessments for downstream oil palm waste biorefinery. Through the valorization of the biogas (waste) to H_2 production, this study can stand as an integrated starting point in bridging both the catalyst preparation and DRM process to support the realization of a circular economy.

2. METHODOLOGY

Figure 2a shows the research flow adopted for the work, including techno-economic, environmental, and sensitivity

https://doi.org/10.1021/acsomega.1c06873
ACS Omega 2022, 7, 15369−15384

analyses to investigate the most feasible Ni-based catalysts in industrial-scale DRM. The descriptions of each step are presented in the following subsections.

2.1. Model Development. The data collection was performed and adopted in DRM (see descriptions in Supporting Information Section S-1). From Table 2, five types of Ni-based catalysts were identified based on a similar production scale (lab scale) and the same type of feedstock (CH_4 and CO_2) and operation mode (batch process). This is to ensure that the comparative study can be made based on a fair basis.

Table 2. Ni-Based Catalysts Considered in This Comparative Study

Ni-based catalyst	remarks	source
Ni-MOF	Ni impregnated on metal−organic framework (MOF), MIL-53(Al)	25
Ni-Ce/Al_2O_3	bimetallic catalyst, Ni (10 wt %) and Ce (5 wt %) with alumina (Al_2O_3) as support	19
Ni/Al_2O_3	conventional catalyst, Ni (10 wt %) with alumina (Al_2O_3) support	19
Ni-HTNT	Ni impregnated on protonated titanate nanotube (HTNT) as support	34
Ni	unsupported Ni catalyst	35

The DRM model was simulated using Aspen Plus V12, which comprises three main units, namely, biogas treatment, reformer, and syngas (mainly CO and H_2) cleaning (see Figure 2b).[36,37] The feed biogas composition was adopted from Shahidul et al.[38] as shown in Table 3. On the other hand, based on Figure 2b, various equipment is needed in the DRM plant, in which the corresponding details are listed in Table 4. In this work, a custom pressure swing adsorber (PSA) MATLAB model was developed and connected with the Aspen Plus V12 (see Figure 2c) using COM technology (i.e., a toolbox that enables the integration of interfaces between MATLAB and Aspen Plus). This is essentially part of the model to simulate H_2 purification more accurately rather than the conventional method of relying on an assumed separation efficiency (typically 98−99%).[39]

Table 3. Composition of biogas[38]

element	composition range (vol%)	composition (vol%) used in model development
CH_4	50−75	50
CO_2	25−45	45
H_2O	2−7	4.75
O_2	<2	0.05
N_2	<2	0.05
H_2S	<2	0.05
NH_3	<1	0.05
H_2	<1	0.05
	Total:	100

2.1.1. Biogas Treatment. Biogas treatment mainly aims at removing H_2S before entering the reformer as the presence of H_2S will cause adverse effects on the DRM process, specifically on the DRM efficiency, syngas purity, pipeline clogging, and catalysts' life span (due to rapid deactivation).[41] Fe_2O_3 was selected as the adsorbent to remove the H_2S given its capability of reducing the H_2S down to the ppm level and its affordable nature.[40,42] During the desulfurization process, Fe_2O_3 will react with unwanted H_2S to form iron sulfide (FeS) (see eq 1). In the subsequent stage, Fe_2O_3 can be regenerated from FeS *via* a thermal oxidation process (see eq 2). The amount of Fe_2O_3 required was calculated using the "calculator" function in Aspen Plus using a Fortran statement, as shown in eq 3. Generally, 250 g of Fe_2O_3 was required for 36 L/min of biogas feed, reducing 3000 ppm of H_2S to 50 to 100 ppm.[40] Similarly, the amount of O_2 required for regeneration was also written as a Fortran statement (see eq 4).

$$Fe_2O_3 + H_2S + 2H_2 \rightarrow FeS + 3H_2O \quad (1)$$

$$2FeS + 7/2O_2 \rightarrow Fe_2O_3 + 2SO_2 \quad (2)$$

$$F_{CATALYST} = (F_{BIOGAS} \div \rho_{BIOGAS} \times 1000/60) \times 0.25 \div 36 \quad (3)$$

where $F_{CATALYST}$ refers to the amount of Fe_2O_3 needed (kg) and F_{BIOGAS} is the molar flow of biogas (kmol/h), while ρ_{BIOGAS}, on the other hand, denotes the molar density of biogas (kmol/m^3).

$$F_{OXYGEN} = F_{FES} \div 2 \times 3.5 \quad (4)$$

where F_{OXYGEN} refers to the molar flow of O_2 needed (kmol/h), while F_{FES} indicates the molar flow of FeS formed through eq 1 (kmol/h).

2.1.2. Reformer. Due to the lack of kinetics information on Ni-based catalysts in the literature, the DRM process cannot be modeled using R_{Plug} in Aspen Plus V12. Therefore, the R_{Yield} block was used instead, where the CH_4 and CO_2 conversion

Table 4. Major Equipment Used in the DRM Model Development

unit	equipment	operating condition	remarks
biogas treatment	desulfurization unit (DESULF) *(RStoic)*	temperature: 450 °C pressure: 22.29 bar[40]	to remove H_2S before entering the reformer with iron(III) oxide (Fe_2O_3) as adsorbent
	regeneration unit (REGEN) *(RStoic)*	temperature: 650 °C pressure: 20.22 bar[40]	to regenerate iron sulfide (FeS) back to Fe_2O_3 to be reused
reformer	reformer (REFORMER) *(User2)*	temperature: MOF: 650 °C Ni-HTNT & Ni: 700 °C Ni-Ce/Al_2O_3 & Ni/Al_2O_3: 800 °C pressure: 1.01 bar	main reaction of DRM where CH_4 and CO_2 are converted to produce CO and H_2
syngas cleaning	separator (S-102) *(Flash2)*	temperature: 180 °C pressure: 6.22 bar	to remove excess water from product
	pressure swing adsorption (PSA) *(User2)*	temperature: 25 °C pressure: 6.5 bar	to adsorb other impurities (N_2, CH_4, CO_2, and CO) to produce high purity of H_2

https://doi.org/10.1021/acsomega.1c06873
ACS Omega 2022, 7, 15369−15384

rates, along with H_2 and CO yields, were obtained from the literature and inserted into the block.[19,25,34,35] To ensure the high reliability and accuracy of the results, the mass balance calculation was performed using a User2 block function in Aspen Plus V12 that was interconnected to the Excel spreadsheet (i.e., material balance calculation).[43] The information related to the inlet flow of the reformer was first imported into the remote Excel spreadsheet. With the aid of the Macro function, the material balance of each component was conducted, while the obtained outlet flow can then be subsequently exported back into the Aspen model to proceed with the subsequent simulation.

2.1.3. Syngas Cleaning. The products exiting from the reformer (i.e., CH_4, CO_2, H_2O, O_2, N_2, H_2S, NH_3, CO, and H_2) were introduced into the syngas cleaning process. This unit generally aims to remove the impurities and enhance the purity of the H_2 product. A phase separator was used to remove the excess water as a significant amount of water was produced from the reformer. In addition, the PSA system was used to eliminate other undesired gases. PSA is the most used conventional technique due to its competitive potential to filter out impurities down to ppm in the production of high purity of 99.99% H_2.[44] Instead of assuming the separation efficiency of PSA, this work attempted to estimate the separation efficiency of the PSA system using mathematical programming *via* MATLAB R2019b. As mentioned earlier, Aspen Plus and MATLAB were interconnected through Microsoft Excel (see Figure 2c).[39] The MATLAB codes were written with considerations of the Languir−Freundlich isotherm parameter, loading ratio correlation (LRC) model, and linear driving force (LDF) model coefficients (see detailed information in Supporting Information Section S-2).[45] In addition, the dual-layer adsorbents zeolite 5A (Z5A) and activated carbon (AC) were used as the adsorbent due to their respective characteristics, where Z5A can adsorb traces of CO and N_2, while AC removes a bulk amount of CO_2 and CH_4.[46] The parameters used to model the PSA system are listed in Table 5. Note that the detailed parameters, density, and void fraction of the opted adsorbents (in this work, Z5A and AC adsorbents are selected) can be found in Supporting Information Section S-2.

Table 5. Parameters Used for PSA System Model Development

parameters	value
bed volume ratio (Z5A:AC)	3:7[47]
total length of bed	4.8 m[39]
adsorption time	180 s[47]
interstitial velocity	0.45 m/s[39]
inlet temperature	25 °C[39]
inlet pressure	6.5 bar[47]

2.2. Techno-economic Analysis. A techno-economic analysis was performed thoroughly to evaluate the economic viability of the Ni-based catalysts in the DRM process (inclusive of biogas treatment, reformer, and syngas cleaning), including the investment costs of the catalyst synthesis process and the DRM process. In general, catalyst synthesis costs involve raw material cost (mass loss during the synthesis process was neglected), utility cost, and capital cost of equipment, while the DRM process cost encompasses both utility cost and capital cost. It is worth noting that the capital cost of the DRM process was obtained from the economic analyzer in Aspen Plus V12.

The DRM plant was assumed to have a life span of 20 years, including 1.5 years of commissioning (70% in the first year and 30% in the second year), with an annual operating time of 8000 h. The other expenses also included operation cost, maintenance cost, operating overhead, property taxes, insurance, as well as general expenses. On the other hand, income tax and depreciation were also considered in this techno-economic analysis (see Supporting Information Section S-3). The techno-economic analysis was carried out assuming that the plant location is in Malaysia where the cost (and emissions) parameters required for the analyses are obtained based on the collected regional data (see Supporting Information Sections S-9 and S-11).

To evaluate the economic performance, various economic indicators including net present value (NPV), payback period (PBP), return of investment (ROI), and discounted cash flow rate of return (DCFRR) were applied in this study (see equations in Supporting Information Section S-4).

2.3. Environmental Analysis. In view of the growing concerns in environmental protection and responsible production, it is essential to ensure the environmental sustainability of the H_2 production process. With this, the environmental analysis was performed to evaluate the environmental impact of each Ni-based catalyst in terms of the overall carbon emissions of the green H_2 production (involved the catalyst synthesis process and DRM process while excluding those attributed by transportation), where the boundary was considered to be a cradle-to-gate analysis. In terms of the catalyst synthesis process, the emission factor attributed[48−58] to raw materials and utility used were considered, whereas for the DRM process, the emissions were mostly attributed to the emitted gaseous products (e.g., CH_4, CO_2, and H_2O), utility consumption, and the use of adsorbents (see equations in Supporting Information Section S-5).

2.4. Sensitivity Analysis. Sensitivity analysis is essential to examine the uncertainties in forecasting the viability of a project.[59] For example, the unit prices of H_2, raw materials, and utilities are subjected to market fluctuations from time to time. This analysis can also provide insights on the robustness of the obtained results. In general, throughout the sensitivity analysis, the techno-economic analysis will be reperformed multiple times by varying the value of each cost parameter (i.e., (i) H_2 price, (ii) raw material cost, and (iii) utility cost).

3. RESULTS AND DISCUSSION

As mentioned in Section 2.3, this study focuses on the investment cost in two aspects: (i) the catalyst synthesis process and (ii) the DRM process. The economic performance is presented in the following subsections.

3.1. Catalyst Synthesis Cost. In terms of the cost associated with the catalyst synthesis process, it encompasses various cost items, including raw material cost, utility cost, and capital cost for catalyst synthesis.

3.1.1. Raw Material Cost. The raw material cost concerns the procurement cost of the materials required for the Ni-based catalyst synthesis process. The amount of raw materials required for each Ni-based catalyst is summarized in Supporting Information Section S-6. Based on the results shown in Figure 3a, the raw material cost required to synthesize the Ni-based MOF catalyst was the highest among the five Ni-based catalysts. This was attributed to the intensive raw material cost used for washing agents (to remove unwanted residue completely), particularly the *N*,*N*-dimethylformamide (DMF). Since it

https://doi.org/10.1021/acsomega.1c06873
ACS Omega 2022, 7, 15369−15384

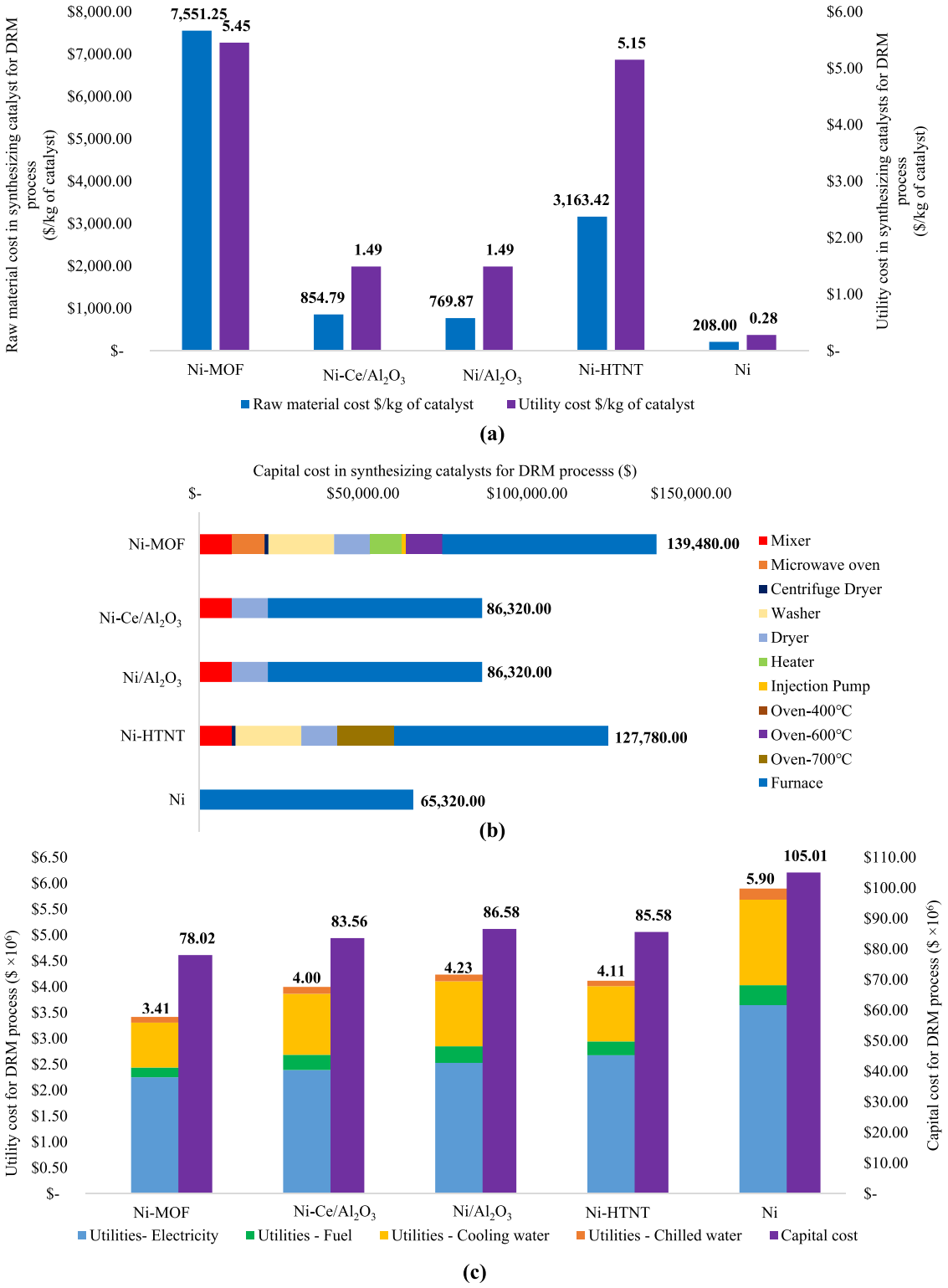

Figure 3. (a) Raw material cost and utility cost required for Ni-based catalysts' synthesis. (b) Capital cost for equipment used in synthesizing Ni-based catalysts. (c) Utility cost and capital cost for different Ni-based catalysts in the DRM process. *Note: Costings were calculated based on a plant scale of 10 tonnes H_2 per day.

required a significant amount of DMF in the synthesis process (i.e., about 180.57 L/kg of the Ni-MOF catalyst), the material costs were therefore boosted up. It was then followed by Ni-HTNT where the high-cost nature was mainly due to its requirement of various types of raw materials (e.g., sodium hydroxide, titanium dioxide, hydrochloric acid, nickel(II) nitrate hexahydrate, and deionized water). Subsequently, Ni-Ce/Al_2O_3 and Ni/Al_2O_3 required less raw material costs given the much simpler process. Generally, the former has a relatively higher raw material cost that was attributed to the additional cerium(III) nitrate hexahydrate, $Ce(NO_3)_3{\cdot}6H_2O$, added to form the

https://doi.org/10.1021/acsomega.1c06873
ACS Omega 2022, 7, 15369−15384

Table 6. Performance of Ni-Based Catalysts in the DRM Process

catalyst	performance			feed flow rate (kmol/h)	amount of catalyst (kg)[d]	energy efficiency (%)[e]
	CH_4 conversion	CO_2 conversion	H_2/CO ratio			
Ni-MOF[25]	74 mol %	80 mol %	1.03	277.8	296.2	36.46%
Ni-Ce/Al_2O_3[19]	82 mol %	88 mol %	0.87[a]	308.4	917.5	35.59%
Ni/Al_2O_3[19]	76 mol %	78 mol %	0.85[b]	336.5	1000.9	33.07%
Ni-HTNT[34]	75 mol %	70 mol %	0.80	349.7	471.6	32.13%
Ni[35]	45 mol %	65 mol %	0.72[c]	504.3	1242.4	21.40%

[a]Calculated using a 1.35 H_2 yield and 1.55 CO yield. [b]Calculated using a 1.23 H_2 yield and 1.45 CO yield. [c]Calculated using a 40 mol % H_2 yield and 55 mol % CO yield. [d]Calculated with a target H_2 production of 10 tonnes per day. [e]Calculated with the percentage of energy produced over energy consumed, evaluated on the basis of the higher heating value (HHV).

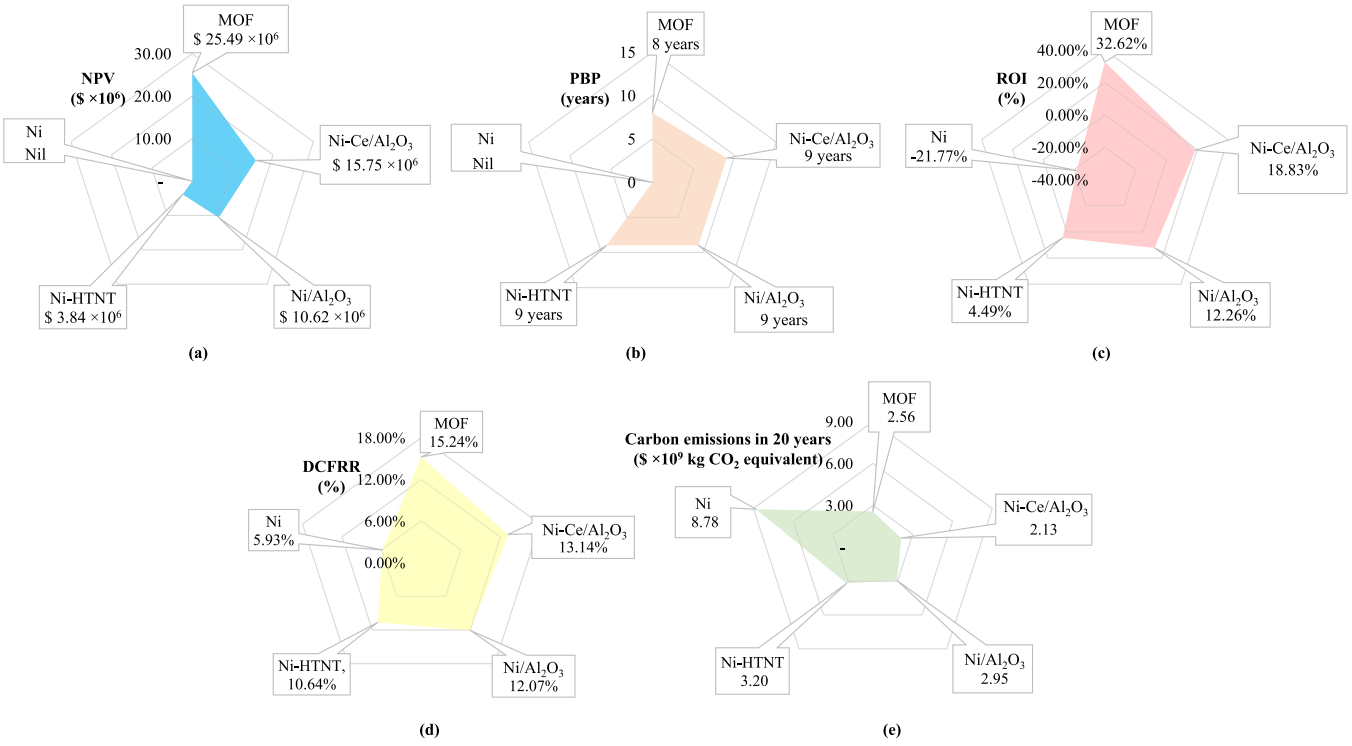

Figure 4. Performances of various Ni-based catalysts in terms of (a) NPV, (b) PBP, (c) ROI, (d) DCFRR, and (e) environmental performance (carbon emissions in 20 years).

bimetallic catalyst. Lastly, Ni had the least cost as it was directly sourced without the need for other raw materials.

3.1.2. Utility Cost. The utility cost mainly considers the total amount of energy consumed during the catalyst's synthesis process such as the drying, washing, and impregnation method. The detailed calculations are attached in Supporting Information Section S-9. Based on Figure 3a, Ni-MOF and Ni-HTNT required a high utility cost given their complex synthesis process. For instance, the microwave-assisted method that required high energy consumption was required to synthesize the MOF-support for Ni-MOF (13.5 MJ/kg Ni-MOF). On the other hand, Ni-HTNT possesses a high energy cost due to its sophisticated synthesis method that required a long synthesis time (128 h). It was then followed by Ni-Ce/Al_2O_3 and Ni/Al_2O_3, while the Ni had the least utility cost as it only involves catalyst activation.

3.1.3. Capital Cost. Figure 3b shows the capital cost needed in the catalyst's synthesis process for each Ni-based catalyst (see Supporting Information Section S-10). As mentioned, the synthesis of both Ni-MOF and Ni-HTNT contains a series of processes (i.e., drying, mixing, washing, centrifuging, incipient wetness impregnation, calcination, and reduction) that, therefore, lead to a higher capital cost. The capital cost required for the case of the Ni-MOF catalyst and Ni-HTNT is about 61.58% and 44.56% more expensive than that for Ni-Ce/Al_2O_3 and Ni/Al_2O_3. On the other hand, these cases were about 113.53% (Ni-MOF) and 91.03% (Ni-HTNT) more expensive than that of unsupported Ni case since the synthesis processes of the former two catalysts were relatively more complex (Ni-Ce/Al_2O_3 and Ni/Al_2O_3 were synthesized using incipient wetness impregnation, while pure Ni only required preactivation).

3.2. DRM Process. This section covers the cost associated under the DRM process. In general, the catalytic performance of the catalysts (see Table 6) will influence the magnitude of the investment cost in the DRM process. For example, given a H_2 production goal of 10 tonnes per day, the catalyst with a lower catalytic performance will lead to a greater requirement of the biogas feed. This further leads to a greater energy consumption, which then results in a lower energy efficiency. Additionally, the overall utility cost and capital cost were expected to be higher than that of the catalysts with better catalytic performance. The corresponding utility cost and capital cost for each Ni-based

https://doi.org/10.1021/acsomega.1c06873
ACS Omega 2022, 7, 15369−15384

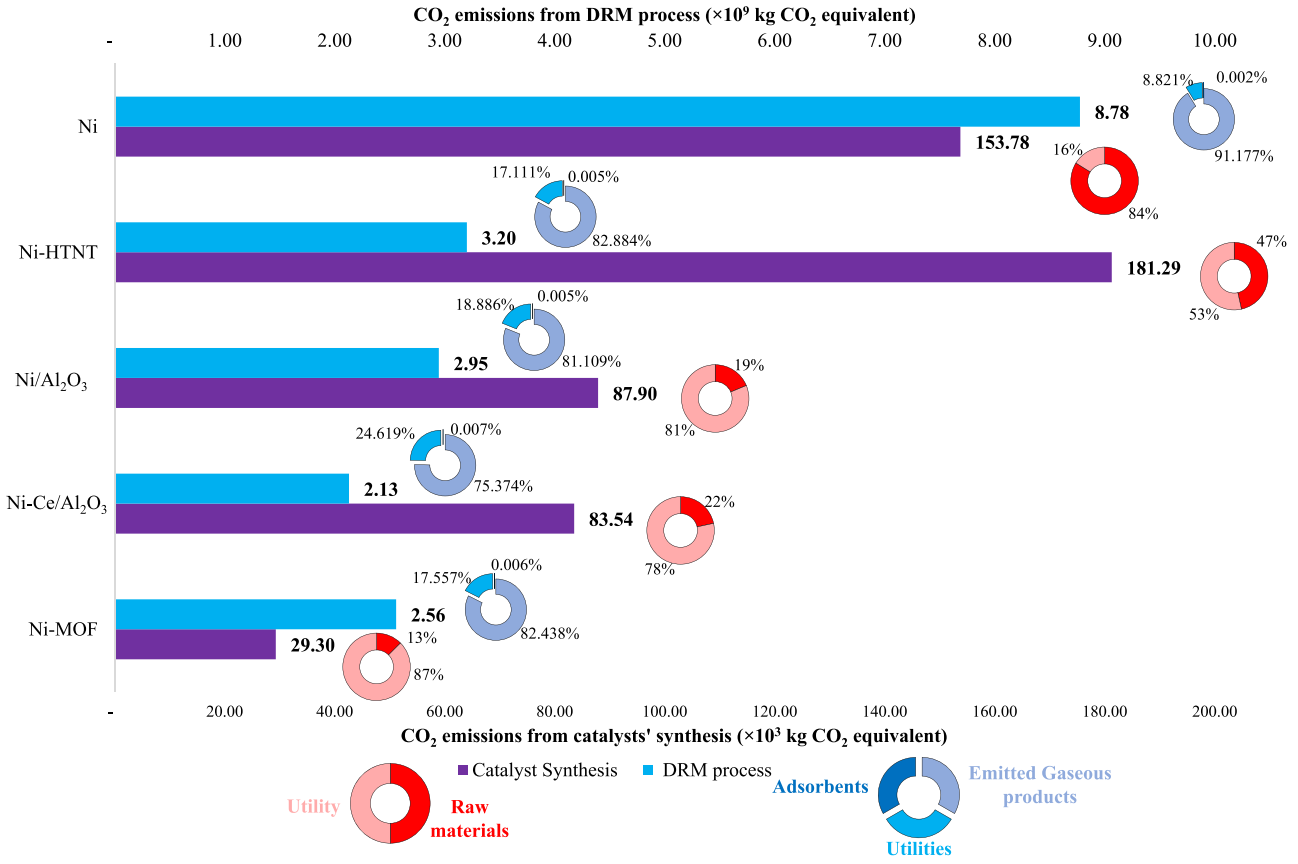

Figure 5. Carbon emissions from the Ni-based catalyst synthesis and DRM process.

catalyst are presented in the following subsections. It is worth noting that the raw material cost was omitted since the biogas was assumed to be sourced from POME that is generally free of charge.

3.2.1. Utility Cost. The utility costs in the DRM process for different Ni-based catalysts are portrayed in Figure 3c. As mentioned, the amount of utilities required is proportionate to the feed flow rate. Therefore, Ni that had the poorest performance requires the highest biogas feed (81.53% more than Ni-MOF) among the Ni-based catalysts (see Table 6). This further leads to a greater consumption rate of utility in the DRM process (i.e., 72.67% greater than that of Ni-MOF). Nevertheless, despite better performance from Ni-Ce/Al_2O_3 and Ni/Al_2O_3, the utility cost was about the same as that of Ni-HTNT. This was due to the fact that the optimal operating temperature of the reformer that utilizes Ni-Ce/Al_2O_3 and Ni/Al_2O_3 is about 800 °C, which is much higher than that of other Ni-based catalysts (e.g., the operating condition for the DRM process that utilizes Ni-HTNT and Ni is 750 °C). Ni-MOF incurred the lowest utility cost due to its high catalytic performance and lower requirement of optimal operating temperature for the reformer (i.e., 650 °C). It is worth noting that the utility cost is mainly attributed to the electricity consumption (about 61% to 66%) that is the major utility used in the DRM process, followed by cooling utility (about 28% to 33%) and heating utility (about 5% to 8%) (see calculations in Supporting Information Section S-11).

3.2.2. Capital Cost. Similarly, the capital cost for the DRM process is subjected to the feed flow rate (greater feed that leads to the need for a larger equipment size). For example, to achieve a H_2 production rate of 10 tonnes per day, the capital cost for the DRM process that utilized Ni-MOF was 25.71% less than that of the DRM process that used Ni as the catalysts, given that the biogas feed for Ni-MOF was only 44.91% of Ni. It is worth noting that, due to the high operating temperature for Ni-Ce/Al_2O_3 and Ni/Al_2O_3, the associated capital costs have become even higher (stainless steel 321 was selected as the construction material to withstand the operating condition) (see calculations in Supporting Information Section S-12).

3.3. Economic and Environmental Performance. This section outlines the overall performances in both economic and environmental aspects. Figure 4 summarizes the performances (in terms of four economic indicators and one environmental indicator) of each Ni-based catalyst, which are further discussed in the subsequent subsections:

3.3.1. Economic Performance. The economic performances of different Ni-based catalyst applications were evaluated to identify the most economically feasible catalysts for H_2 production *via* the DRM process. The economic performances were analyzed, while corresponding cash flow statements are tabulated in Supporting Information Section S-15. The economic indicators that were used to evaluate the economic performance include, NPV, PBP, ROI, and DCFRR.

In this work, the NPV of the plant in 20 years was evaluated based on the investment cost estimated in Section 3.1. Based on Figure 4a, the DRM with Ni-MOF offered the highest NPV value of $25.49 million. This was due to the greater catalytic performance of Ni-MOF as compared to other Ni-based catalysts (see Table 6). This somehow revealed the potential of using Ni-MOF in green H_2 production in an industrial DRM plant. In contrast, the use of unsupported Ni as the DRM catalysts led to a negative NPV value of −$22.88 million. This

https://doi.org/10.1021/acsomega.1c06873
ACS Omega 2022, 7, 15369−15384

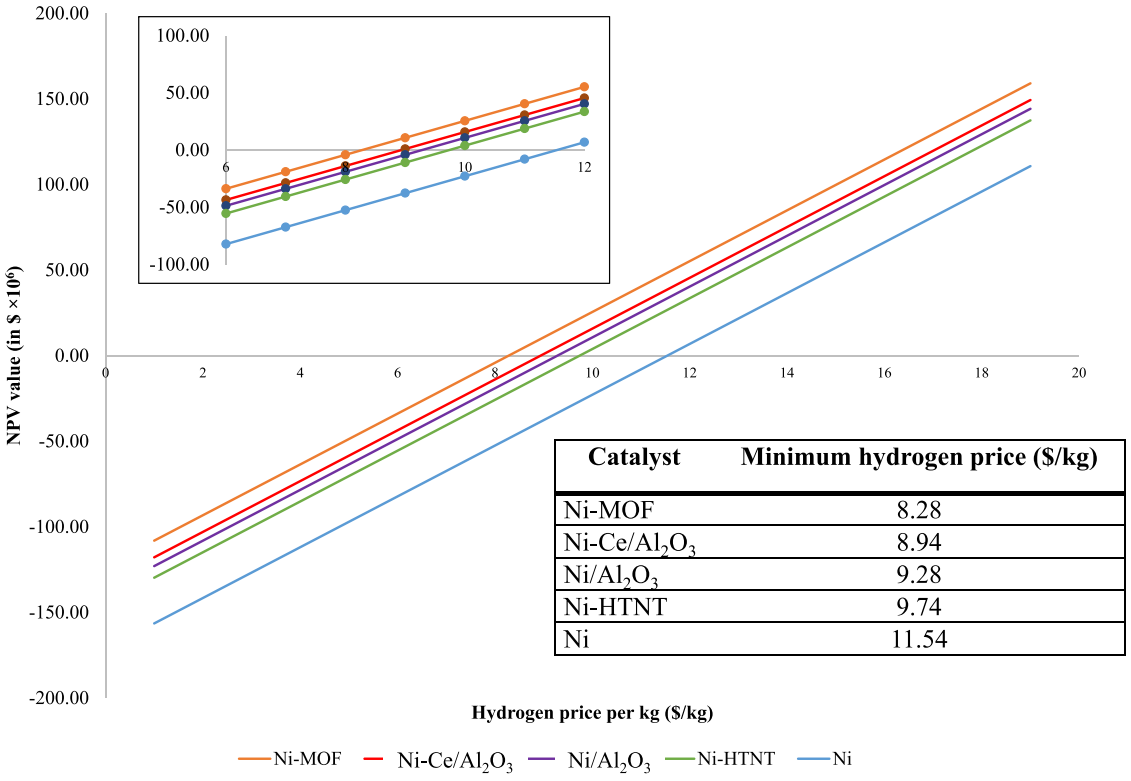

Catalyst	Minimum hydrogen price ($/kg)
Ni-MOF	8.28
Ni-Ce/Al_2O_3	8.94
Ni/Al_2O_3	9.28
Ni-HTNT	9.74
Ni	11.54

Figure 6. Trend of NPV value (in $ × 10^6) of different Ni-based catalysts at different H_2 unit prices.

showed that the revenue obtained from the H_2 sale could not compensate for the large investment costs (revenue is 3.22% less than the total investment cost required) incurred in the unsupported Ni case.

In addition to a high NPV, a good project should come with a reasonably short PBP. This indicates that it is more desirable if the amount of time required to recoup the investment cost is shorter. In fact, having a long PBP may cause the economic feasibility to become unsecured due to the uncertainties in the distant future. As illustrated in Figure 4b, a reasonable PBP of 8 to 9 years was obtained for the case of Ni-MOF, Ni-Ce/Al_2O_3, and Ni/Al_2O_3, while the use of Ni-HTNT may prolong the PBP to about 10 years given that the production cost of Ni-HTNT was much higher (270% to 310% higher than Ni-Ce/Al_2O_3 and Ni/Al_2O_3) while having a similar number of catalyst life span (4 years) as Ni-Ce/Al_2O_3 and Ni/Al_2O_3 (3 years).

On the other hand, ROI was used to evaluate the investment potential and economic performances.[60] As expected, the higher ROI (32.62%) was dedicated to Ni-MOF, which was 2.66-fold compared to the conventional Ni/Al_2O_3 (see Figure 4c). It was followed by Ni-Ce/Al_2O_3, which can only offer a ROI (18.83%) that was almost half of the one offered by Ni-MOF.

Generally, the use of all Ni-based catalysts (except for the unsupported Ni case) can lead to a decent DCFRR of more than 10% (see Figure 4d). Nevertheless, Ni-MOF, which offers the highest DCFRR (15.24%), still stood out from the rest. This further confirms that it is worthful to consider investing and commercializing the use of Ni-MOF for sustainable H_2 production.

Note that a negative NPV was obtained for the unsupported Ni case, in which a negative ROI of −21.77% was experienced. Therefore, it was unable to pay back within the 20-year time frame (PBP = ″nil″). On the other hand, given that the use of Ni-MOF requires the shortest PBP and was capable of offering the highest NPV, ROI, and DCFRR, its overall economic viabilities over other Ni-based catalysts can be justified.

3.3.2. Environmental Performance. As shown in Figure 4e, the environmental performance (in terms of the total carbon emissions for a plant life span of 20 years) of each Ni-based catalyst in green H_2 production was evaluated from the total emitted gaseous products, utilities, adsorbent application, and Ni-based catalysts used (see Supporting Information Sections S-16 to S-19). As shown, Ni-Ce/Al_2O_3 had the lowest carbon emissions (2.13 × 10^9 kg CO_2 equivalent), which is 16.71% lower than that of the Ni-MOF case (2.56 × 10^9 kg CO_2 equivalent) (see Figure 5). As expected, due to the poor catalytic performance of the unsupported Ni catalyst, it offered the greatest carbon emissions among all studied Ni-based catalysts. The distribution of the carbon emissions (in the catalyst synthesis process and DRM process) is shown in the subsections below.

3.3.2.1. Carbon Emissions from Catalyst Synthesis. The carbon emissions from catalyst synthesis were from the emission factors of the raw materials used and from the energy consumption during the synthesis of the Ni-based catalysts. To note, the total emissions were also subjected to their respective regeneration life span. For instance, Ni-Ce/Al_2O_3, which had a life span of 3 years, would need to be regenerated six times throughout the 20 year life span. In other words, the total emissions will need to account for six regeneration cycles (i.e., the number of regeneration activities needed within the 20 year plant life span).

On the other hand, based on Figure 5, the carbon emissions to synthesize Ni-MOF catalysts were mainly contributed by utility consumption (note that the energy source here refers to the energy mix of the studied area, inclusive of natural gas, coal, and oil[55]) from the catalyst synthesis process (87%). This was due to the DMF washing agent having a relatively low emission

https://doi.org/10.1021/acsomega.1c06873
ACS Omega 2022, 7, 15369−15384

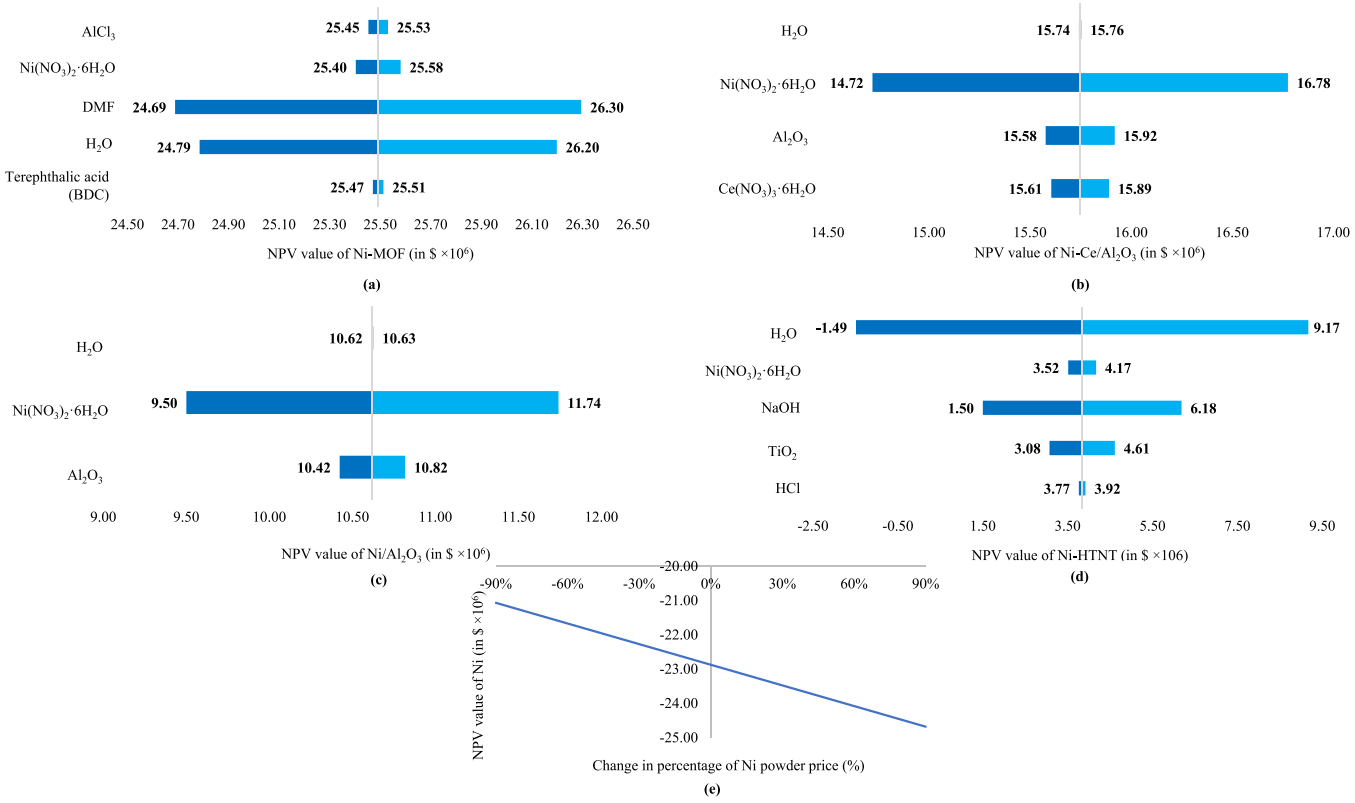

Figure 7. Sensitivity analysis on the raw material price of different Ni-based catalysts: (a) Ni-MOF, (b) Ni-Ce/Al_2O_3, (c) Ni/Al2O_3, (d) Ni-HTNT, and (e) Ni.

factor.[50] Similarly, in Ni-Ce/Al_2O_3 and Ni/Al_2O_3 cases, the carbon emissions were mainly contributed by the energy consumption, i.e., about 78% and 81%, respectively, whereas for the Ni-HTNT case, the total carbon emissions were 117% of Ni-Ce/Al_2O_3, where the emissions were fairly distributed across both raw materials (contributed 47%) and utility consumption (contributed 53%). It is worth noting that the emission factor of NaOH used in Ni-HTNT synthesis process was relatively high, i.e., up to 1.12 kg CO_2/kg of NaOH.[48] In contrast, the emissions for the unsupported Ni case were mainly attributed to the material (84%) given that the synthesis process of these catalysts only requires a single step, i.e., the activation process.

3.3.2.2. Carbon Emissions from the DRM Process. The carbon emissions from the DRM process have accounted for the emissions from the gaseous products in the DRM process (e.g., CH_4, CO_2, and H_2O), utilities, and adsorbents used. For the emissions caused by the products, Ni-Ce/Al_2O_3 had the least contribution due to its high CH_4 and CO_2 conversion. As observed in Figure 5, the gaseous products are the main contributors (>70%) to the overall carbon emissions from the DRM process. Furthermore, the carbon emissions attributed to utilities were found to be directly proportional to the energy consumption of each Ni-based catalyst. Generally, catalysts with the best catalytic performance (i.e., Ni-MOF) will require the lowest total energy consumption, thus leading to the lowest carbon emissions (4.49×10^6 kg CO_2 equivalent) among the studied Ni-based catalysts. The adsorbents used in the DRM process include Fe(III) oxide (for H_2S removal) and Z5A and AC (for H_2 purification). Note that the emission contribution from adsorbents is relatively low (1.50×10^5 kg CO_2 equivalent in 20 years, which is ~99.97% lower than that of the energy consumption) as the regeneration only takes every 5 years.

3.4. Sensitivity Analysis. The sensitivity analysis was carried out to identify the impact of various preassumed parameters on the NPV estimation. The investigated parameters include (i) H_2 price, (ii) raw material cost (for catalysts), and (iii) utility cost.

3.4.1. H_2 Price. The base H_2 price used in the techno-economic analysis was assumed to be $10/kg. In this sensitivity analysis, the price was varied from −90% to 90% of the current assumed price. This not only helps decision-makers to identify the minimum H_2 price that the plant can be sustained without a loss in profit but also serves as a guide for investors to gauge the risk associated with the fluctuation of the H_2 price in the market.

Figure 6 illustrates the changes in NPV against the H_2 price (ranging from $1 to $19/kg). Generally, a higher H_2 selling price will lead to a greater revenue of the green H_2 plant. For instance, when the H_2 was sold at $19/kg, the NPV obtained from the Ni-MOF case can increase to 159.07×10^6. The minimum H_2 price is extracted and summarized in the table shown in Figure 6. As expected, given the superior economic performance of the Ni-MOF case, it offers the lowest minimum H_2 selling price (i.e., $8.28/kg) among others. This indicates that the plant will be generating profit as long as the H_2 price was kept above $8.32/kg. In contrast, the NPV of the poorest unsupported Ni catalysts will maintain positive only if the H_2 was sold at price greater than $11.54/kg (see calculations in Supporting Information Section S-21).

3.4.2. Raw Material Price. Due to the possible occurrence of fluctuation in the raw material price, this section aims to investigate the sensitivity of the unit price of each key raw material on the obtained NPV of the respective Ni-based catalysts.

https://doi.org/10.1021/acsomega.1c06873
ACS Omega 2022, 7, 15369−15384

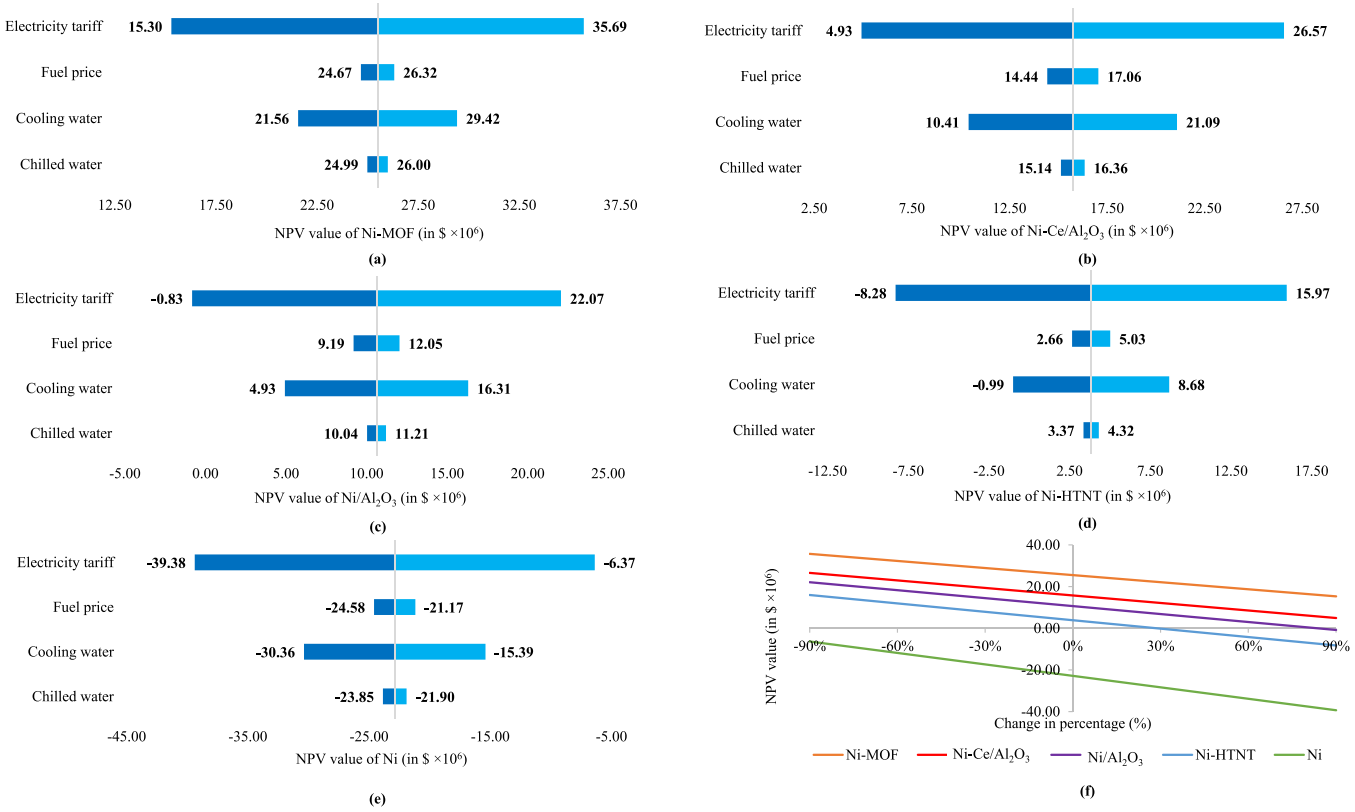

Figure 8. Sensitivity analysis on the utility price with application of different Ni-based catalysts: (a) Ni-MOF, (b) Ni-Ce/Al_2O_3, (c) Ni/Al_2O_3, (d) Ni-HTNT, and (e) Ni. (f) Trend of NPV against variation in electricity tariff.

From Figure 7, the most sensitive parameter for Ni-MOF synthesis was the DMF price. This is due to the high-cost nature of DMF where the unit cost price of DMF in the base case was \$18.70/L.[61] In addition, DMF was highly required in synthesizing and washing the Ni-MOF catalyst (180.57 L/kg catalyst synthesized). Meanwhile, for the synthesis of Ni-Ce/Al_2O_3 and Ni/Al_2O_3, the most sensitive parameter was the Ni precursor ($Ni(NO_3)_2{\cdot}6H_2O$) price. This is because the Ni precursor had a slightly higher unit cost price as compared to the other raw materials such as alumina (the unit cost of the Ni precursor is 9.32 times higher than that of alumina). On the other hand, the most sensitive parameter for the Ni-HTNT was the unit cost of deionized water, given its high-volume requirement (112.79 L/kg catalysts synthesized).

Furthermore, the unsupported Ni catalyst simply required Ni powder for the synthesis process. Therefore, the sensitivity analysis was carried out to evaluate the impact of the fluctuation in Ni powder price on the NPV (see Figure 7e). Nevertheless, although the unit price of Ni powder had been reduced by 90%, the NPV still remained negative. This shows that the gigantic investment cost could not be compensated with the low unit price of the Ni powder (see calculations in Supporting Information Section S-22).

3.4.3. Utility Price. This subsection, on the other hand, investigates the impact of the unit cost of various utilities (i.e., electricity tariff, fuel price, cooling water, and chilled water cost) on the attained NPV. The results are illustrated in Figure 8.

From Figure 8, it is clearly seen that the electricity tariff had the greatest impact on the NPV of the plant for all Ni-based catalysts (i.e., the greatest deviation shown in the tornado chart). Therefore, the sensitivity of the electricity tariff was further investigated (see Figure 8e).

Figure 8 shows that the use of both the Ni-MOF catalyst and bimetallic catalyst (Ni-Ce/Al_2O_3) was capable of providing a positive NPV even when the electricity tariff was increased by 90%. This showed the robustness of this DRM plant. Meanwhile, for Ni/Al_2O_3, the impact of electricity tariff on the NPV was more significant as it will turn negative if the electricity tariff was increased by 83.49%. Moreover, given the high energy requirement of Ni-HTNT, a slight increment of the electricity tariff (28.53%) will lead to a negative NPV. Lastly, for the unsupported Ni catalyst case, the NPV still remained negative even though the electricity tariff had been reduced by up to 90%. This further confirmed the infeasibility of using unsupported Ni as the DRM catalyst.

Among the sensitivity analyses, it was discovered that the changes in H_2 selling price have the greatest impact as compared to fluctuations of raw material price and utility price. This shows the importance of securing the selling price of green hydrogen on promoting the deployment of the catalytic DRM process for green hydrogen production. As proven in previous sections, the plant only showed a positive NPV when the H_2 selling price had increased by 15.41% or more; however, it suffered a loss even when the raw material price and utility price had dropped to 90% for the unsupported Ni case (see calculations in Supporting Information Section S-23).

3.5. Additive Manufacturing. Additive manufacturing (or known as 3D printing) is a cutting-edge technology to fabricate bulk production of objects precisely and effectively in a short period of time.[62,63] Lately, 3D printing technology had been acknowledged as a paradigm in fabricating the complex design of a catalyst in mass production, offering an attractive means of forming structured metal−organic frameworks (MOFs), since it enables precise and accurate customization and tailoring on

https://doi.org/10.1021/acsomega.1c06873
ACS Omega 2022, 7, 15369−15384

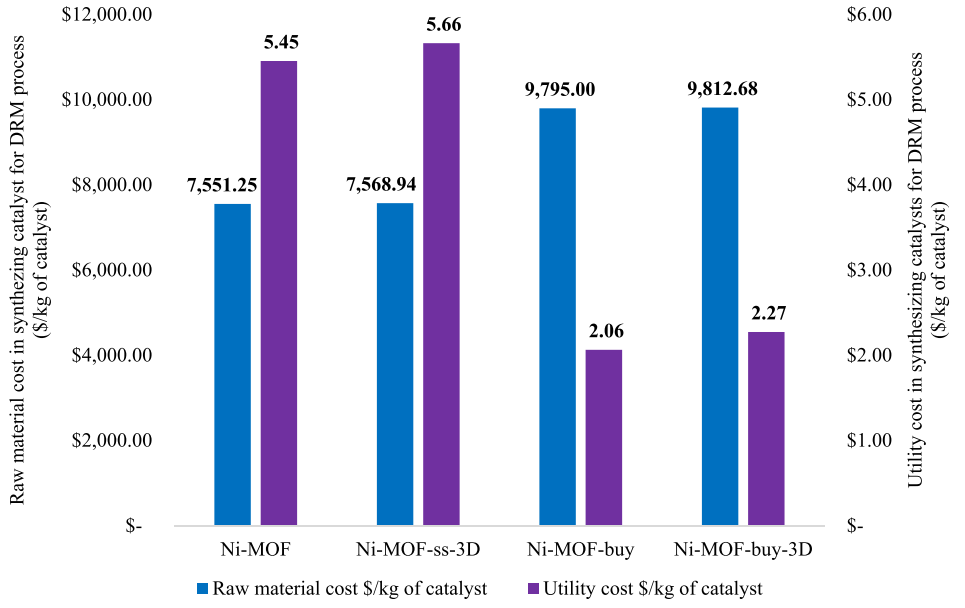

(a)

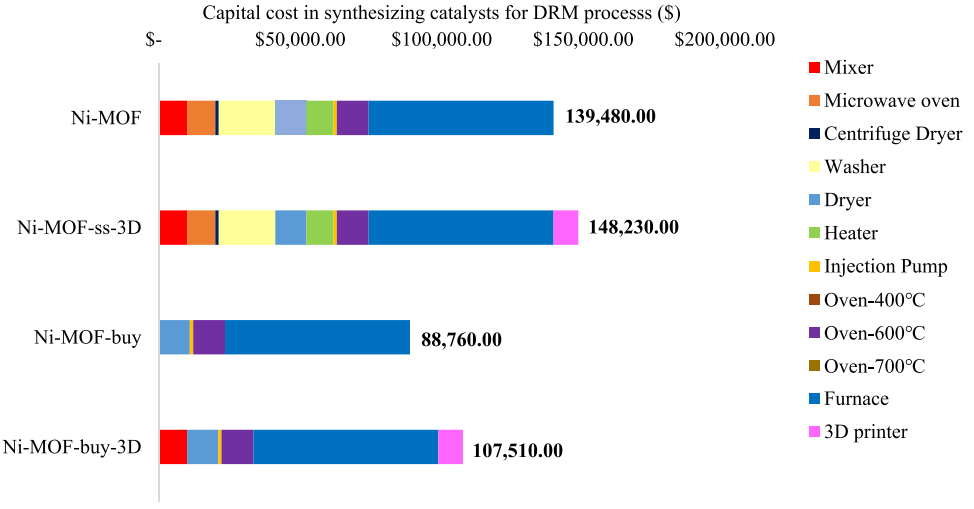

(b)

Figure 9. (a) Raw material cost and utility cost required for MOF-based catalyst synthesis. (b) Capital cost for equipment used in synthesizing MOF-based catalysts.

geometry and molecule structures.[64,65] However, this technology is still at its infant stage due to the lack of sustainability and feasibility studies that impedes its attractiveness in the catalytic-centric energy system.

Based on the findings above (Sections 3.1 to 3.3), it was shown that Ni-MOF had the best performance in both economic and environmental aspects. Therefore, this section aimed to discover the robustness of 3D printing for the bulk production of Ni-MOF catalysts. After thorough consideration, the four different approaches that may vary its overall feasibility were chosen as shown:

1. MOF support was synthesized using the microwave-assisted method, while Ni was impregnated onto MOF using the wet incipient impregnation method (labeled as Ni-MOF).
2. MOF was synthesized using the microwave-assisted method, while Ni was impregnated onto the MOF support using the 3D printing method (labeled as Ni-MOF-ss-3D)
3. MOF was purchased directly from the market, while Ni was impregnated onto MOF using the wet incipient impregnation method (labeled as Ni-MOF-buy)
4. MOF support was purchased directly from the market, while Ni was impregnated using the 3D printing method (labeled as Ni-MOF-buy-3D)

The comparison study in terms of economic and environmental performances of each synthetic strategy focused on the catalyst synthesis process only since it will not cause any effects on the DRM process.

3.5.1. Investment Cost. Based on Figure 9a, the raw material cost for purchasing the parent MOF (MIL-53(Al)) was

https://doi.org/10.1021/acsomega.1c06873
ACS Omega 2022, 7, 15369−15384

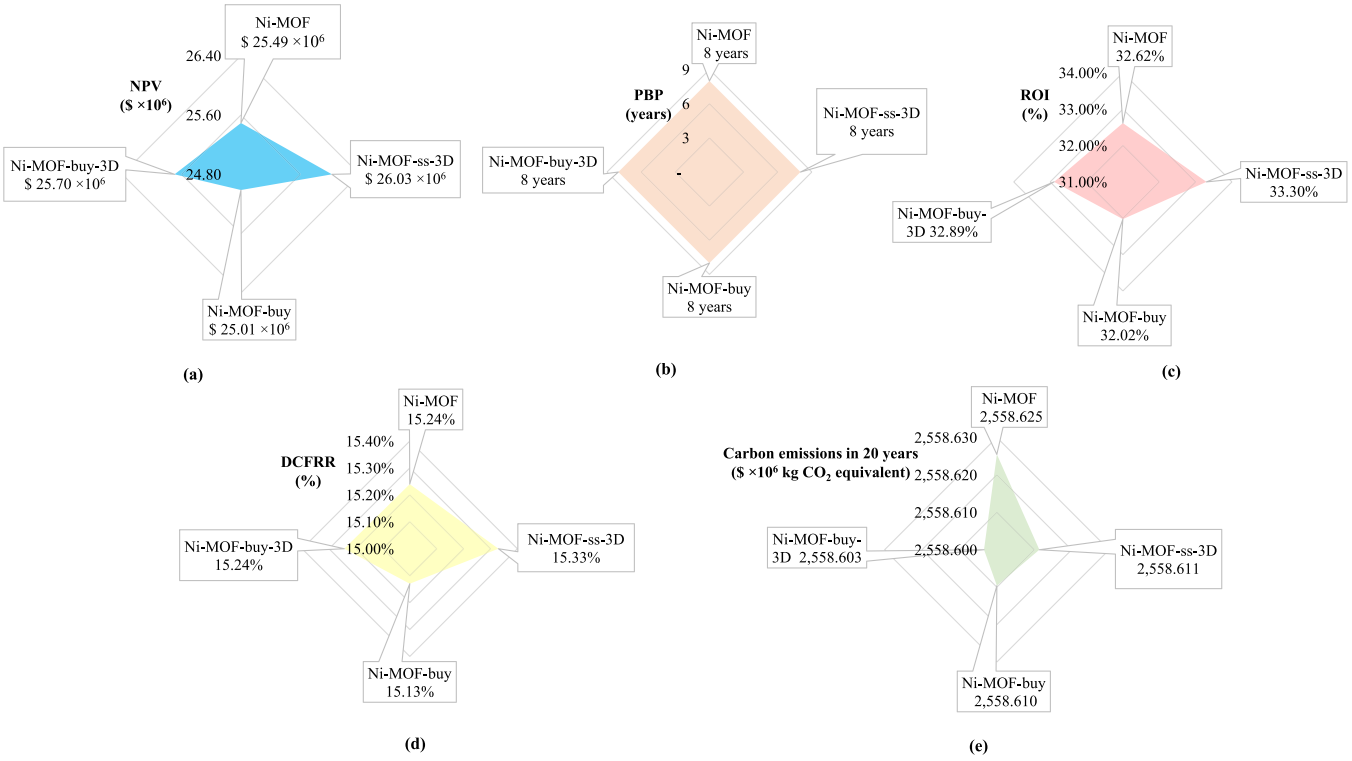

Figure 10. Comparison of different MOF-based catalysts in aspects of (a) NPV, (b) ROI, (c) DCFRR, and (d) environmental performance (carbon emissions in 20 years).

significantly higher due to the high unit cost of MIL-53(Al) (around $3105/kg).[66] In addition, the raw material cost for the 3D printing method was also higher than that of the conventional method; this was due to the addition of binders (e.g., polyvinyl alcohol and bentonite clay) required for paste densification and formation of elastic paste rheology to ease the 3D printing process.[67]

On the other hand, when the parent MOF (MIL-53(Al)) was purchased, the utility consumption for MOF synthesis was no longer required where the parent MOF purchased was readily available. Therefore, this led to a significantly lower utility cost (about 58 to 64% lower than the other two cases: Mi-MOF and Ni-MOF-ss-buy). On the other hand, the use of the 3D printing method had increased the utility cost by 3% to 11% as it involved an additional 3D printer. The additional equipment of a 3D printer had increased the energy consumption (8.1 MJ/kg of catalysts synthesized) as compared to the conventional method.

As illustrated in Figure 9b, the capital cost for the cases of purchasing the parent MOF was almost halved as compared to others given the simplification of the synthetic process. Similarly, due to the need for an additional 3D printer, the capital cost for synthesizing the catalyst *via* the 3D printing method was slightly higher (6.27% higher for Ni-MOF-ss-3D as compared to Ni-MOF) than that of the conventional method.

3.5.2. Economic and Environmental Performance. The corresponding economic and environmental performances were estimated and are summarized in Figure 10.

The NPV obtained from MOF-based catalysts synthesized *via* the 3D printing method was about 2% to 3% higher than that of the conventional method. This is due to the longer life span (about twofold as compared to the conventional method[68]). Given the same reason, Ni-MOF-ss-3D was capable of offering the greatest ROI and DCFRR among all cases. Besides, after accounting for all the investment cost items as shown in Section 3.4.1, purchasing the MOF parent directly from the market will generally lead to a poorer economic performance (e.g., the NPV obtained from Ni-MOF-buy was 1.87% lower than that of the Ni-MOF case). It is worth noting that all four cases were capable of paying back during the eighth year.

In terms of the environmental aspect, Ni-MOF-buy-3D had contributed the least carbon emissions followed by Ni-MOF-ss-3D (see Figure 10e). This is because Ni-MOF-buy-3D does not take into consideration the carbon emissions from synthesizing the parent MOF. Due to the longer catalyst life span (about twofold longer than that of the catalysts synthesized from the conventional method), the use of the 3D printing method had proved its capability to be environmentally friendly by emitting less CO_2 within the 20 year life span (e.g., shifting Ni-MOF to Ni-MOF-ss-3D can reduce about 14,117.03 kg CO_2 equivalent).

In short, there is a bright future in the bulk production of MOF-based catalysts *via* additive manufacturing. This is due to its accuracy of printing where organic linkers and precursors can be printed at their respective coordinates more precisely, creating a completely homogeneous packing arrangement where the position and orientation alignment of particles are highly accurate according to a prior design, ensuring its superior catalytic performance.[69] The current proposed model implied the manufacturing in a scaled-up quantity (10 kg) where it could be improved by manufacturing on a larger scale to save utility cost and energy consumption.

4. CONCLUSIONS

The valorization of biogas in H_2 production *via* the DRM process is subtle as a golden opportunity to convert "waste" into "wealth", at the same time reducing carbon emissions gradually. Among the five Ni-based catalysts, the MOF-based catalyst had

https://doi.org/10.1021/acsomega.1c06873
ACS Omega 2022, 7, 15369−15384

proved its feasibility in terms of both economic (NPV of $25.49 × 10^6) and environmental (total carbon emissions of $2.56 × 10^9 kg CO_2 equivalent) aspects on a 20 year basis. Nevertheless, this work had shown the capability of an advanced synthetic method, the 3D printing method, in enhancing the overall economic (NPV is 2.10% better than that of the conventional microwave-assisted method) and environmental performances (14,117.03 kg CO_2 less than that of the conventional method). In summary, this work has concluded that:

1) Based on the five proposed Ni-based catalysts in the DRM process, the economic and environmental performance rankings are listed as follows: Ni-MOF > Ni-Ce/Al_2O_3 > Ni/Al_2O_3 > Ni-HTNT > unsupported Ni.

2) The analyses had proved the infeasibility of unsupported Ni (conventional industrial catalyst) in DRM that incurs a large investment cost.

3) The additive manufacturing technique (3D printing) offers a better sustainability performance in terms of both economic and environmental aspects since it can produce MOF that had a longer life span as compared to the conventional technique.

4) From the sensitivity analyses, the H_2 price had the most significant impact than the raw material price and utility price. Thus, decision-makers should consider this factor thoughtfully when venturing into such proposed sustainable hydrogen production business.

These insights are beneficial for the future process engineer in commercializing the MOF-based catalytic DRM process that is deemed as an attractive way to achieve the greening of various H_2 sink industries (e.g., including oil and gas sectors). The subsequent works can expand the study scope to cover other resource conservation alternatives (e.g., consideration of the salvage value of metal that can be recovered from the spent catalysts) and process integration techniques (e.g., heat integration to enhance energy recovery).

■ ASSOCIATED CONTENT

Supporting Information

The Supporting Information is available free of charge at https://pubs.acs.org/doi/10.1021/acsomega.1c06873.

All the calculations from the catalyst synthesis to the DRM process, inclusive of techno-economic and environmental analyses, and the figures and charts that explain the sensitivity analyses carried out (PDF)

■ AUTHOR INFORMATION

Corresponding Author

Bing Shen How − *Biomass Waste-to-Wealth Special Interest Group, Research Centre for Sustainable Technologies, Faculty of Engineering, Computing and Science, Swinburne University of Technology, 93350 Kuching, Sarawak, Malaysia;* orcid.org/0000-0002-0969-9167; Email: bshow@swinburne.edu.my

Authors

Jia Ling Ong − *Biomass Waste-to-Wealth Special Interest Group, Research Centre for Sustainable Technologies, Faculty of Engineering, Computing and Science, Swinburne University of Technology, 93350 Kuching, Sarawak, Malaysia*

Adrian Chun Minh Loy − *Department of Chemical and Biological Engineering, Monash University, Clayton, VIC 3800, Australia*

Sin Yong Teng − *Institute for Molecules and Materials, Radboud University, 6500 GL Nijmegen, the Netherlands;* orcid.org/0000-0002-2988-8053

Complete contact information is available at: https://pubs.acs.org/10.1021/acsomega.1c06873

Notes

The authors declare no competing financial interest.

■ ACKNOWLEDGMENTS

The authors would like to acknowledge the financial support from the Ministry of Higher Education under the Fundamental Research Grant Scheme (grant FRGS/1/2020/TK0/SWIN/03/3) and Swinburne University of Technology Sarawak Campus via the Early Career Researcher Award (2-5704) and Research Success Award (2-5747).

■ ABBREVIATIONS

AC, activated carbon; DCFFR, discounted cash flow rate of return; DMF, *N*,*N*-dimethylformamide; DRM, dry methane reforming; HTNT, protonated titanate nanotube; LDF, linear driving force; LRC, loading ratio correlation; MOF, metal−organic framework; NPV, net present value; PBP, payback period; POME, palm oil mill effluent; PSA, pressure swing adsorption; ROI, return of investment; SDG, sustainable development goals; Z5A, zeolite 5A

■ REFERENCES

(1) Jiao, Y.; Su, H.; Hou, W.; Liao, Z. A Multiperiod Optimization Model for Hydrogen System Scheduling in Refinery. *Ind. Eng. Chem. Res.* **2012**, *51*, 6085−6098.

(2) Jin, B.; Ye, X.; Zhong, H.; Jin, F. Light-Driven Hydrogenation of Bicarbonate into Formate over Nano-Pd/TiO2. *ACS Sustainable Chem. Eng.* **2020**, *8*, 6798−6805.

(3) Yang, Y.; Xue, Y.; Huang, F.; Zhang, H.; Tao, K.; Zhang, R.; Shen, Q.; Chang, H. A Facile Microfluidic Hydrogen Peroxide Fuel Cell with High Performance: Electrode Interface and Power-Generation Properties. *ACS Appl. Energy Mater.* **2018**, *1*, 5328−5335.

(4) McDonald, J. M., Andrew Global hydrogen demand expected to drop in 2020 due to pandemic: Platts Analytics. https://www.spglobal.com/platts/en/market-insights/latest-news/electric-power/051420-global-hydrogen-demand-expected-to-drop-in-2020-due-to-pandemic-platts-analytics (accessed 26 September 2021).

(5) Sönnichsen, N. *Global hydrogen production 2018 & 2030.* https://www.statista.com/statistics/1121207/global-hydrogen-production/ (accessed 26 September 2021).

(6) *IEA The Future of Hydrogen.* https://www.iea.org/reports/the-future-of-hydrogen (accessed 26 October 2020).

(7) *United Nations #Envision2030: 17 goals to transform the world for persons with disabilities.* https://www.un.org/development/desa/disabilities/envision2030.html (accessed 15 November 2020).

(8) *International Production Assessment Division Palm Oil Explorer.* https://ipad.fas.usda.gov/cropexplorer/cropview/commodityView.aspx?cropid=4243000(accessed 23 August 2021).

(9) Chin, S. Y.; Shahruddin, S.; Chua, G. K.; Samsodin, N.; Setiabudi, H. D.; Karam Chand, N. S.; Chew, F. N.; Leong, J. X.; Jusoh, R.; Samsudin, N. A. Palm Oil-Based Chemicals for Sustainable Development of Petrochemical Industries in Malaysia: Progress, Prospect, and Challenges. *ACS Sustainable Chem. Eng.* **2021**, *9*, 6510−6533.

(10) Hosseini, S. E.; Abdul Wahid, M. Pollutant in palm oil production process. *J. Air Waste Manage. Assoc.* **2015**, *65*, 773−781.

(11) Rahayu, A. S.; Karsiwulan, D.; Yuwono, H.; Trisnawati, I.; Mulysari, S.; Rahardjo, S.; Hokermin, S.; Paramita, V. *Handbook: POME-to-Biogas: Project Development in Indonesia.* https://winrock.org/wp-content/uploads/2016/05/CIRCLE-Handbook-2nd-Edition-

EN-25-Aug-2015-MASTER-rev02-final-new02-edited.pdf (accessed 25 October 2021).
(12) Tan, Y. D.; Lim, J. S. Feasibility of palm oil mill effluent elimination towards sustainable Malaysian palm oil industry. *Renewable Sustainable Energy Rev.* **2019**, *111*, 507−522.
(13) Kim, T.-H.; Lee, K.; Kim, M. Y.; Chang, Y. K.; Choi, M. Effects of Fatty Acid Compositions on Heavy Oligomer Formation and Catalyst Deactivation during Deoxygenation of Triglycerides. *ACS Sustainable Chem. Eng.* **2018**, *6*, 17168−17177.
(14) Luna-Murillo, B.; Pala, M.; Paioni, A. L.; Baldus, M.; Ronsse, F.; Prins, W.; Bruijnincx, P. C. A.; Weckhuysen, B. M. Catalytic Fast Pyrolysis of Biomass: Catalyst Characterization Reveals the Feed-Dependent Deactivation of a Technical ZSM-5-Based Catalyst. *ACS Sustainable Chem. Eng.* **2021**, *9*, 291−304.
(15) Wang, Y.; Yao, L.; Wang, Y.; Wang, S.; Zhao, Q.; Mao, D.; Hu, C. Low-Temperature Catalytic CO2 Dry Reforming of Methane on Ni-Si/ZrO2 Catalyst. *ACS Catal.* **2018**, *8*, 6495−6506.
(16) Lyu, Y.; Jocz, J.; Xu, R.; Stavitski, E.; Sievers, C. Nickel Speciation and Methane Dry Reforming Performance of Ni/CexZr1−xO2 Prepared by Different Synthesis Methods. *ACS Catal.* **2020**, *10*, 11235−11252.
(17) He, X.; Liu, L. Thermodynamic analysis on the CO 2 conversion processes of methane dry reforming for hydrogen production and CO 2 hydrogenation to dimethyl ether. *IOP Conf. Ser.: Earth Environ. Sci.* **2017**, *100*, 012078.
(18) García-Diéguez, M.; Pieta, I. S.; Herrera, M. C.; Larrubia, M. A.; Alemany, L. J. Nanostructured Pt- and Ni-based catalysts for CO2-reforming of methane. *J. Catal.* **2010**, *270*, 136−145.
(19) Chein, R.-Y.; Fung, W.-Y. Syngas production via dry reforming of methane over CeO2 modified Ni/Al2O3 catalysts. *Int. J. Hydrogen Energy* **2019**, *44*, 14303.
(20) Fischer, F.; Tropsch, H. The composition of products obtained by the petroleum synthesis. *Brennst. Chem.* **1928**, *39* ().
(21) Dias, J. A.; Assaf, J. Influence of calcium content in Ni/CaO/γ-Al2O3 catalysts for CO2-reforming of methane. *Catal. Today* **2003**, *85*, 59−68.
(22) Guo, J.; Lou, H.; Zhao, H.; Wang, X.; Zheng, X. Novel synthesis of high surface area MgAl2O4 spinel as catalyst support. *Mater. Lett.* **2004**, *58*, 1920−1923.
(23) Liu, D.; Lau, R.; Borgna, A.; Yang, Y. Carbon dioxide reforming of methane to synthesis gas over Ni-MCM-41 catalysts. *Appl. Catal., A* **2009**, *358*, 110−118.
(24) Coelho, D. C.; Oliveira, A. C.; Filho, J. M.; Oliveira, A. C.; Lucredio, A. F.; Assaf, E. M.; Rodríguez-Castellón, E. Effect of the active metal on the catalytic activity of the titanate nanotubes for dry reforming of methane. *Chem. Eng. J.* **2016**, *290*, 438−453.
(25) Karam, L.; Reboul, J.; Casale, S.; Massiani, P.; El Hassan, N. Porous Nickel-Alumina Derived from Metal-Organic Framework (MIL-53): A New Approach to Achieve Active and Stable Catalysts in Methane Dry Reforming. *ChemCatChem* **2020**, *12*, 373−385.
(26) Śliwa, E. I.; Nesterov, D. S.; Kirillova, M. V.; Kłak, J.; Kirillov, A. M.; Smoleński, P. A 3D MOF based on Adamantoid Tetracopper(II) and Aminophosphine Oxide Cages: Structural Features and Magnetic and Catalytic Properties. *Inorg. Chem.* **2021**, *60*, 9631−9644.
(27) Mallakpour, S.; Azadi, E.; Hussain, C. M. MOF/COF-based materials using 3D printing technology: applications in water treatment, gas removal, biomedical, and electronic industries. *New J. Chem.* **2021**, *45*, 13247−13257.
(28) Pascanu, V.; González Miera, G.; Inge, A. K.; Martín-Matute, B. Metal−Organic Frameworks as Catalysts for Organic Synthesis: A Critical Perspective. *J. Am. Chem. Soc.* **2019**, *141*, 7223−7234.
(29) Wei, Y.-S.; Zhang, M.; Zou, R.; Xu, Q. Metal−Organic Framework-Based Catalysts with Single Metal Sites. *Chem. Rev.* **2020**, *120*, 12089−12174.
(30) Khan, I. S.; Ramirez, A.; Shterk, G.; Garzón-Tovar, L.; Gascon, J. Bimetallic Metal-Organic Framework Mediated Synthesis of Ni-Co Catalysts for the Dry Reforming of Methane. *Catalysts* **2020**, *10*, 592−592.
(31) Khani, Y.; Kamyar, N.; Bahadoran, F.; Safari, N.; Amini, M. M. A520 MOF-derived alumina as unique support for hydrogen production from methanol steam reforming: The critical role of support on performance. *Renewable Energy* **2020**, *156*, 1055−1064.
(32) Imyen, T.; Znoutine, E.; Suttipat, D.; Iadrat, P.; Kidkhunthod, P.; Bureekaew, S.; Wattanakit, C. Methane Utilization to Methanol by a Hybrid Zeolite@Metal−Organic Framework. *ACS Appl. Mater. Interfaces* **2020**, *12*, 23812−23821.
(33) Chin, K. C.; Leong, L. K.; Lu, S.-Y.; Tsai, D.-H.; Sethupathi, S. a. p. Preparation of Metal Organic Framework (MOF) Derived Bimetallic Catalyst for Dry Reforming of Methane. *Int. J. Technol.* **2019**, 1437−1445.
(34) Monteiro, W. F.; Vieira, M. O.; Calgaro, C. O.; Perez-Lopez, O. W.; Ligabue, R. A. Dry reforming of methane using modified sodium and protonated titanate nanotube catalysts. *Fuel* **2019**, *253*, 713−721.
(35) Kennema, M.; Rowntree, P. A. The reactivity and initial carbonization of an Unsupported Nickel catalyst in dry reforming of methane. *J. Power Sources* **2020**, *453*, 226753.
(36) Hernández, B.; Martín, M. Optimal Process Operation for Biogas Reforming to Methanol: Effects of Dry Reforming and Biogas Composition. *Ind. Eng. Chem. Res.* **2016**, *55*, 6677−6685.
(37) Martín, M.; Grossmann, I. E. Energy optimization of bioethanol production via gasification of switchgrass. *AIChE J.* **2011**, *57*, 3408−3428.
(38) Shahidul, M. I.; Malcolm, M. L.; Eugene, J. J. Methane Production Potential of POME: A Review on Waste-to-Energy (WTE) model. *Sci. Int.* **2018**, *30*, 717−728.
(39) Costa, N.; Patrício, P.; Ferreira, R. V.; Neto, M.; Cardoso, M. SIMULATION AND ANALYSIS OF A HYDROGEN GENERATION UNIT. *BJPG* **2018**, *12*, 159−168.
(40) Portzer, J.; Damle, A.; Gangwal, S. *Hot-Gas Desulfurization with Sulfur Recovery*. https://www.osti.gov/servlets/purl/16485 (accessed 3 March 2021).
(41) Stoppacher, B.; Bock, S.; Malli, K.; Lammer, M.; Hacker, V. The influence of hydrogen sulfide contaminations on hydrogen production in chemical looping processes. *Fuel* **2022**, *307*, 121677.
(42) Khabazipour, M.; Anbia, M. Removal of Hydrogen Sulfide from Gas Streams Using Porous Materials: A Review. *Ind. Eng. Chem. Res.* **2019**, *58*, 22133−22164.
(43) *Aspen Plus Aspen Plus Version 10 User Models Reference Manual*. https://sites.chemengr.ucsb.edu/~ceweb/courses/che184b/aspenplus/UserModels.pdf (accessed 15 February 2021).
(44) Bernardo, G.; Araújo, T.; da Silva Lopes, T.; Sousa, J.; Mendes, A. Recent advances in membrane technologies for hydrogen purification. *Int. J. Hydrogen Energy* **2020**, *45*, 7313−7338.
(45) Gratton, A. *Adsorption Modelling - Solving PDE - Axial Dipersion Model*. https://www.mathworks.com/matlabcentral/answers/385756-adsorption-modelling-solving-pde-axial-dispersion-model (accessed 22 March 2021).
(46) Riboldi, L.; Bolland, O. Overview on Pressure Swing Adsorption (PSA) as CO2 Capture Technology: State-of-the-Art. *Energy Procedia* **2017**, *114*, 2390−2400.
(47) Ahn, S.; You, Y.-W.; Lee, D.-G.; Kim, K.-H.; Oh, M.; Lee, C.-H. Layered two- and four-bed PSA processes for H2 recovery from coal gas. *Chem. Eng. Sci.* **2012**, *68*, 413−423.
(48) *Winnipeg Emission factors in kg CO2-equivalent per unit*. https://www.winnipeg.ca/finance/findata/matmgt/documents/2012/682-2012/682-2012_Appendix_H-WSTP_South_End_Plant_Process_Selection_Report/Appendix%207.pdf (accessed 23 November 2020).
(49) Van Uytvanck, P. P.; Haire, G.; Marshall, P. J.; Dennis, J. S. Impact on the Polyester Value Chain of Using p-Xylene Derived from Biomass. *ACS Sustainable Chem. Eng.* **2017**, *5*, 4119−4126.
(50) *Environment Canada Health Canada Priority Substances List Assessment Report- N,N-Dimethylformamdie*. https://www.canada.ca/content/dam/hc-sc/migration/hc-sc/ewh-semt/alt_formats/hecs-sesc/pdf/pubs/contaminants/psl2-lsp2/nnd/nnd-eng.pdf (accessed 1 March 2021).
(51) Nuss, P.; Eckelman, M. J. Life cycle assessment of metals: a scientific synthesis. *PLoS One* **2014**, *9*, e101298−e101298.

https://doi.org/10.1021/acsomega.1c06873
ACS Omega 2022, 7, 15369−15384

(52) EFDB *Emission Factor for CO2 Emissions from Titanium Dioxide Production*. https://www.ipcc-nggip.iges.or.jp/EFDB/find_ef.php?ipcc_code=2.B.6&ipcc_level=2 (accessed 1 March 2021).
(53) Punt, A.; Cunningham, B. E. N. a. E.; SKM Enviros *Quantifying the Carbon Footprint associated with OREX and Textile Garment use in the USA*; 2012.
(54) CETCO *Carbon Footprint Comparison of GCLs and Compacted Clay Liners*. https://www.cetco.com.au/DesktopModules/Bring2mind/DMX/Download.aspx?EntryId=8167&Command=Core_Download&language=en-US&PortalId=31&TabId=3140 (accessed 13 September 2021).
(55) *Isiaka Adeyemi Abdul-Azeez Measuring and Monitoring Carbon Emission to Promote Low-Carbon Development in Johor Bahru*. https://malaysiacities.mit.edu/paperadeyemi#:~:text=Based%20on%20this%20fuel%20mix,Tenaga%20Nasional%20Berhad%20(TNB). (accessed 3 March 2021).
(56) Okitsu, J.; Khamis, M. F. I.; Zakaria, N.; Naono, K.; Haruna, A. A. Toward an architecture for integrated gas district cooling with data center control to reduce CO2 emission. *Sustain. Comput.: Inform. Syst.* **2015**, *6*, 39−47.
(57) Seo, Y.; Suzuki, M.; Takagi, T.; Dowaki, K. Life-Cycle Assessment of Adsorbents for Biohydrogen Production. *Resources* **2019**, *8* ().
(58) Gu, H.; Bergman, R.; Anderson, N.; Alanya Rosenbaum, S. Life cycle assessment of activated carbon from woody biomass. *Wood Fiber Sci.* **2018**, *50*, 229−243.
(59) Sinnott, R. K., *Coulson and Richardson's Chemical Engineering Volume 6 - Chemical Engineering Design (4th Edition)*. Elsevier: 2010.
(60) Fernando, J. *Return of Investment (ROI)*. https://www.investopedia.com/terms/r/returnoninvestment.asp(accessed 29 April 2021).
(61) *Alfa Aeser A13547 N,N-Dimethylformamide, 99%*. https://www.alfa.com/en/catalog/A13547/ (accessed 13 September 2021).
(62) Giubilini, A.; Siqueira, G.; Clemens, F. J.; Sciancalepore, C.; Messori, M.; Nyström, G.; Bondioli, F. 3D-Printing Nanocellulose-Poly(3-hydroxybutyrate-co-3-hydroxyhexanoate) Biodegradable Composites by Fused Deposition Modeling. *ACS Sustainable Chem. Eng.* **2020**, *8*, 10292−10302.
(63) Xu, W.; Wang, X.; Sandler, N.; Willför, S.; Xu, C. Three-Dimensional Printing of Wood-Derived Biopolymers: A Review Focused on Biomedical Applications. *ACS Sustainable Chem. Eng.* **2018**, *6*, 5663−5680.
(64) Liu, W.; Erol, O.; Gracias, D. H. 3D Printing of an In Situ Grown MOF Hydrogel with Tunable Mechanical Properties. *ACS Appl. Mater. Interfaces* **2020**, *12*, 33267−33275.
(65) Shu, J.-C.; Yang, X.-Y.; Zhang, X.-R.; Huang, X.-Y.; Cao, M.-S.; Li, L.; Yang, H.-J.; Cao, W.-Q. Tailoring MOF-based materials to tune electromagnetic property for great microwave absorbers and devices. *Carbon* **2020**, *162*, 157−171.
(66) INSCX *Aluminium Metal Organic Framework (Al-MIL-53), 99%, 30−40μm*. https://inscx.com/shop/product/aluminium-metal-organic-framework-al-mil-53-purity-99-aps-30-40%ce%bcm/ (accessed 13 September 2021).
(67) Lawson, S.; Griffin, C.; Rapp, K.; Rownaghi, A. A.; Rezaei, F. Amine-Functionalized MIL-101 Monoliths for CO2 Removal from Enclosed Environments. *Energy Fuels* **2019**, *33*, 2399−2407.
(68) Alimi, O.; Akinnawo, C.; Meijboom, R. Monolith catalyst design by 3D printing: A reusable support for modern palladium-catalyzed cross-coupling reactions. *New J. Chem.* **2020**, *44*, 18867.
(69) Nawada, S.; Dimartino, S.; Fee, C. Dispersion behavior of 3D-printed columns with homogeneous microstructures comprising differing element shapes. *Chem. Eng. Sci.* **2017**, *164*, 90−98.

https://doi.org/10.1021/acsomega.1c06873
ACS Omega 2022, 7, 15369−15384